A COMPACT LOW-PASS FILTER WITH SHARP CUT-OFF AND LOW INSERTION LOSS CHARACTERISTIC USING NOVEL DEFECTED GROUND STRUCTURE

D. Xi, Y. Z. Yin, L. H. Wen, Y. N. Mo, and Y. Wang

National Laboratory of Antennas and Microwave Technology
Xidian University
Xi'an, Shaanxi 710071, P. R. China

Abstract—In this paper, a compact stepped-impedance hairpin resonator (SIHR) low-pass filter (LPF) with an improved split-ring resonator defected ground structure (ISRR DGS) and two elliptical DGSs is presented. The proposed LPF exhibits the advantages of low insertion loss, sharp cutoff characteristic, wide stopband over the ordinary LPFs. The introduced DGSs are presented to improve the in-band and out-band characteristic. An equivalent RLC circuit model of the two kinds of DGSs is presented and analyzed. Combining with these two structures, a new SIHR LPF having 3 dB cutoff frequency of 2.5 GHz is fabricated and measured. Measured results show that the selectivity of the proposed LPF is more than 100 dB/GHz and the insertion loss is less than 0.5 dB in the passband. A wide stop-band bandwidth with 20 dB attenuation from 2.58 up to 7.5 GHz is achieved. Moreover, the occupied area is only $20 \times 25 \, \text{mm}^2$.

1. INTRODUCTION

Small-size, sharp cutoff characteristic, and low insertion loss low-pass filters (LPFs) are frequently required in many RF and microwave wireless communication systems. Many new types of microstrip filters have been proposed and designed to satisfy these requirements. Due to requirements of miniaturization, low insertion loss and simple structure, defected ground structure (DGS) has become increasingly popular for many microwave circuit designs such as amplifiers, couplers, especially in filters [1–4]. The DGS disturbs the shield current distribution in the ground plane, which can greatly change the

characteristics of a transmission line such as distributed capacitance and inductance. Thus, it can improve passband performances and realize compact size [4, 5].

Another size reduction technology for the resonator, stepped-impedance hairpin resonator (SIHR), has also been dramatically developed [5–8]. However, it has the gradual cutoff skirts and high insertion loss. To improve the cutoff characteristics and the in-band properties, some special DGS cells combined with stepped-impedance hairpin resonator (SIHR) are adopted, which are typically represented by split-ring resonator DGSs and asymmetric DGSs [9, 10].

In this paper, a new design of SIHR LPF is presented. With two elliptical DGSs added to it, the DGSs has good lowpass characteristics and improves the harmonic-suppression characteristic in high frequency stopband. Besides this DGSs structure, an another improved split-ring resonator defected ground structure (ISRR DGS) cell is also incorporated in it, which not only improves the cutoff frequency response but also lowers the insertion loss in the passband. The equivalent circuits of the two kinds of DGS cells are also presented and analyzed. With these structures, the proposed LPF exhibits the characteristic of sharp cutoff characteristic, low insertion loss, wide stopband, compact size and easy fabrication.

2. THE PROPOSED LPF DESIGN

2.1. The SIHR LPF Design

Figure 1 shows the construction of the SIHR. The SIHR consists of a single transmission line L_s and symmetric capacitance-loaded parallel
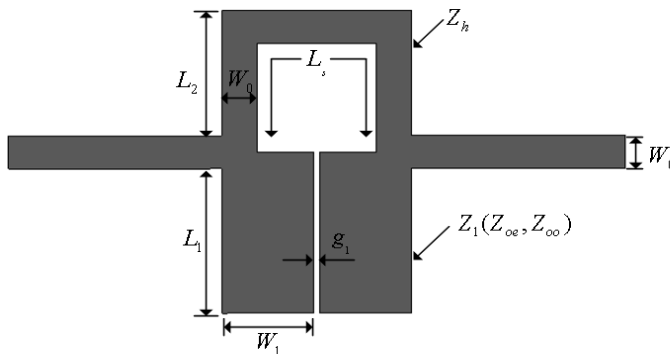
Figure 1. Layout of the SIHR.
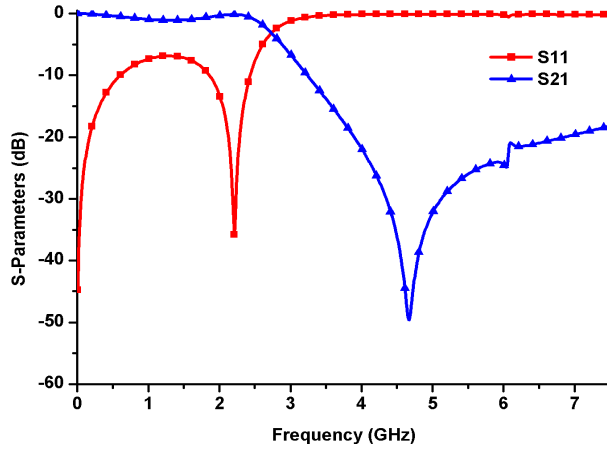
Figure 2. Simulated results of the SIHR LPF.

coupled lines with a length of L_1. Z_h is the characteristic impedance of the single transmission line L_s. Z_{0e} and Z_{0o} are the even-mode and odd-mode impedances of the coupled lines. By properly selecting $Z_h > \sqrt{Z_{0e}Z_{0o}}$, the size of SIHR becomes smaller than that of the conventional hairpin resonator, while it is an elliptic-function low-pass filter using microstrip SIHR [11].

The proposed SIHR LPF is designed for the 3 dB cutoff frequency of 2.5 GHz and fabricated on an F4B-2 substrate of thickness 0.5 mm and relative permittivity $\varepsilon_r = 2.65$. The optimal dimensions of the SIHR LPF are $L_1 = 6$ mm, $L_2 = 5.2$ mm, $W_0 = 1.37$ mm, $W_1 = 3.57$ mm, and $g_1 = 0.5$ mm. Figure 2 shows the simulation results of the SIHR LPF. It shows that the insertion loss is too high and without sharp cutoff skirts out-of-band. In addition, an insufficient attenuation at the stopband better than 20 dB is from 3.63 to 6.17 GHz. To improve the above performance, we introduce two kinds of DGS as followed.

2.2. Elliptical DGS Cell and Equivalent Circuit Analysis

As shown in Figure 3(a), Elliptical DGS cell is obtained by an etched slot, which is connecting with two elliptical defected structures in the ground plane. As is well known, there is a close relationship between the etched sizes of the DGS and electrical parameters of the equivalent element values [12]. To derive the equivalent network parameters, the S-parameters of a DGS cell at the reference plane can
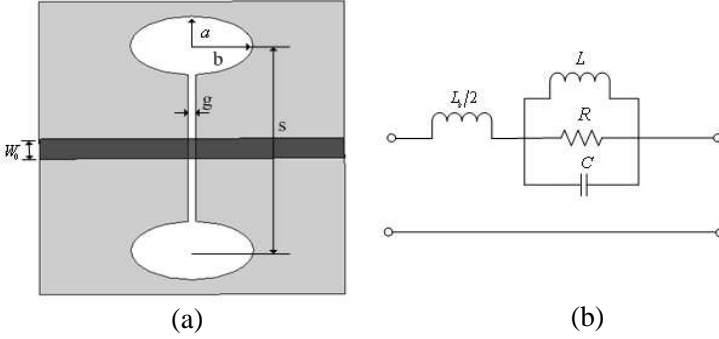
Figure 3. (a) The Elliptical DGS cell and (b) its equivalent circuit.

be calculated by EM-simulator. Then, using the relationship between the S-parameter and ABCD matrix, the equivalent network parameters can be extracted [4].

$$C = \frac{\omega_c}{2Z_0(\omega_0 - \omega_c)} \tag{1}$$

$$L = \frac{1}{4(\pi f_0)^2 C} \tag{2}$$

$$R = \frac{2Z_0}{\sqrt{\frac{1}{|S_{11}(\omega_0)|^2} - (2Z_0(\omega_0 C - \frac{1}{\omega_0 L}))^2 - 1}} \tag{3}$$

where ω_0 is the resonance frequency, ω_c is the 3-dB cutoff frequency, and Z_0 is the characteristic impedance of the microstrip transmission line.

To confirm the validity of the presented equivalent model, the DGS cell has been simulated using HFSS V11.0. For the EM simulation, the permittivity of the dielectric board is 2.65 and its thickness is 0.5 mm, the width of the microstrip transmission line on the top layer is 1.37 mm, which corresponds to the 50 Ω characteristic impedance. The dimension parameters of the DGS cell are $a = 2$ mm, $b = 5$ mm, $s = 14$ mm, and $g = 0.5$ mm. Figure 3(b) shows the equivalent circuit of the proposed DGS cell with equivalent network parameters of $C = 0.9554$ pF, $L = 2.9488$ nH, $R = 1056$ ohm. The comparison showing in Figure 4 reveals that the EM simulation agrees well with the equivalent circuit simulation obtained by advanced design system (ADS).

Figure 5 shows the frequency responses of EM simulation with different radius b. The radius b varies from 3 mm to 5 mm, while the radius $a = 2$ mm, the slot length $s = 14$ mm, and the slot width
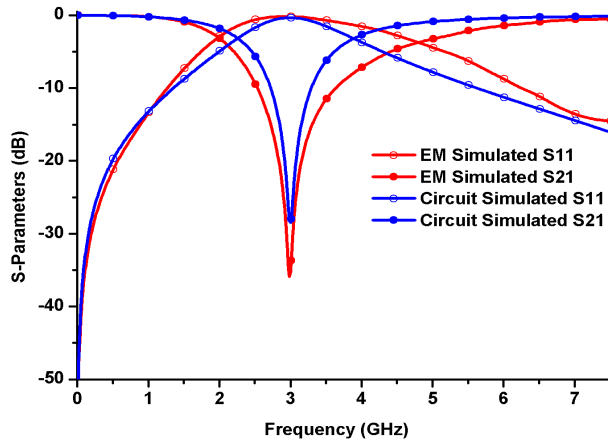
Figure 4. Comparison between the EM and equivalent circuit simulated results.
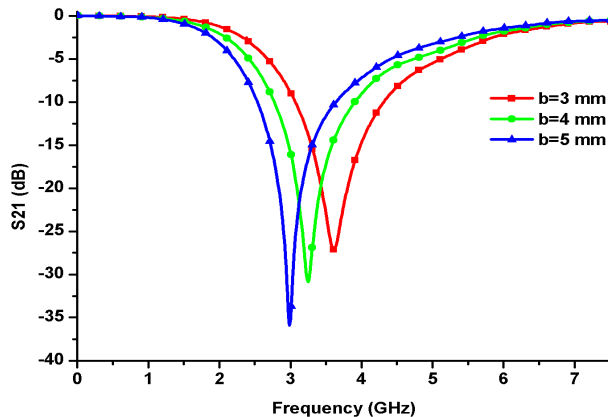
Figure 5. Frequency responses of the elliptical DGS with different radius b.

$g = 0.5\,\text{mm}$ are kept constant. It demonstrates that the value of the inductance L in the equivalent circuit increases as the radius b varies from $3\,\text{mm}$ to $5\,\text{mm}$, which has relatively little effect on the equivalent capacitance C, while both of them can be obtained from the Equations (1) and (2). Simulated results show that the attenuation pole shifts from 3.66 to $3\,\text{GHz}$. This fact indicates that

the equivalent inductance will change as the area of the elliptical DGS varies. Therefore, changing the dimension parameters of the DGS will cause the cutoff frequency and the attenuation poles shift. In other words, the resonant frequency can be controlled by adjusting the elliptical DGS for spurious out-band suppression.

2.3. The ISRR DGS Design and Analysis

As analyzed above, the elliptic DGS can be used for low pass filter design and spurious out-band suppression. However, this structure also has some disadvantages such as insufficient suppression in passband and slow cutoff characteristic. Therefore, an ISRR DGS are introduced into the LPF [13]. Figure 6 shows the proposed structure of the ISRR DGS and its equivalent circuit. It shows that the ISRR DGS functions as a parallel resonator. Therefore, etching split-ring defected structure in the ground means a parallel resonator will be added to the equivalent circuit.

Figure 7 depicts the comparison of three types of different resonators. It shows that the ISRR DGS cell has more advantages over the elliptical DGS cell and conventional complementary split-ring resonator (CSRR) cell, including flatter lowpass property and a sharper cutoff response. Nevertheless, its performance at the stopband becomes worse. Figure 8 shows the variation of the different resonant frequency properties of the ISRR DGS with different radius of R_1. Evidently, the resonant frequency shifts to low frequency band when R_1 gets large, so the resonant frequency can be determined by adjusting the radius R_1 of the ring.

(a)   (b)
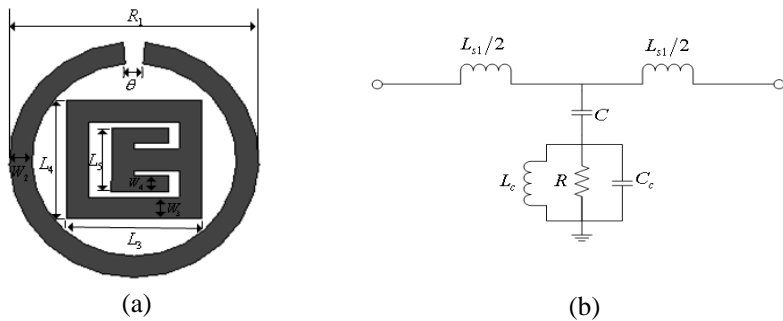
Figure 6. The ISRR DGS (a) layout of the ISRR DGS (b) equivalent circuit model.
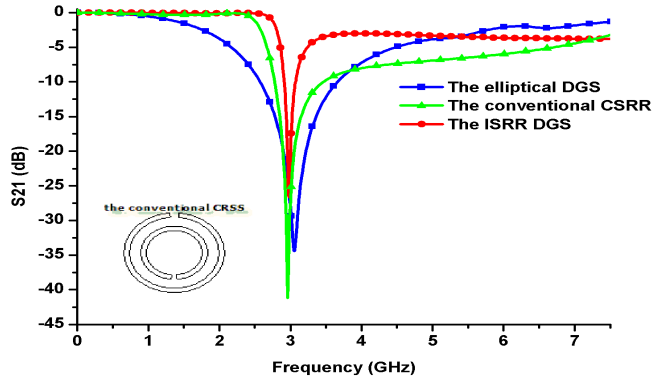
Figure 7. Comparison of the S-parameters properties of the Elliptical DGS cell, the conventional CSRR and the ISRR DGS cell.
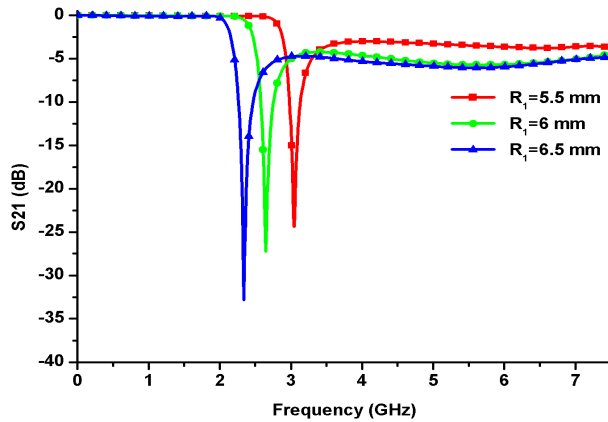
Figure 8. Comparison of the resonant property of different radius R_1.

2.4. The Proposed Lowpass Filter Design and Optimization

Generally, conventional DGS has some disadvantages such as narrow bandwidth at the stopband and insufficient suppression in high-frequency range. In addition, they also have a poor cutoff response. Therefore, to design the desired lowpass filter with compact structure, two elliptical DGSs and an ISRR DGS are introduced into the SIHR LPF to improve the passband insertion loss, cutoff frequency response, and stopband performance.

As shown in the Figure 9, because of the mutual influence of the two kinds of DGS and the electromagnetic field distribution of the SIHR LPF, the distance between the elliptical DGS and the ISRR DGS (L_6) and the distance between the ISRR DGS and the center of the PCB (L_7) should be fine-adjusted to make the filter achieve the best performance. After optimization, the optimal values of the parameters are $a = 0.7\,\text{mm}$, $b = 1.5\,\text{mm}$, $s = 4\,\text{mm}$, $W_0 = 1.37\,\text{mm}$, $W_1 = 3.57\,\text{mm}$, $W_2 = 1\,\text{mm}$, $W_3 = 1\,\text{mm}$, $W_4 = 0.75\,\text{mm}$, $L_1 = 6\,\text{mm}$,
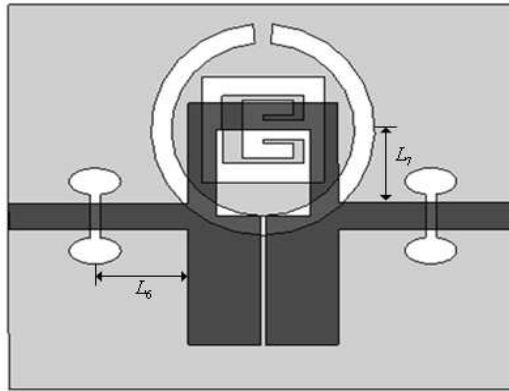
Figure 9. Layout of the proposed LPF.
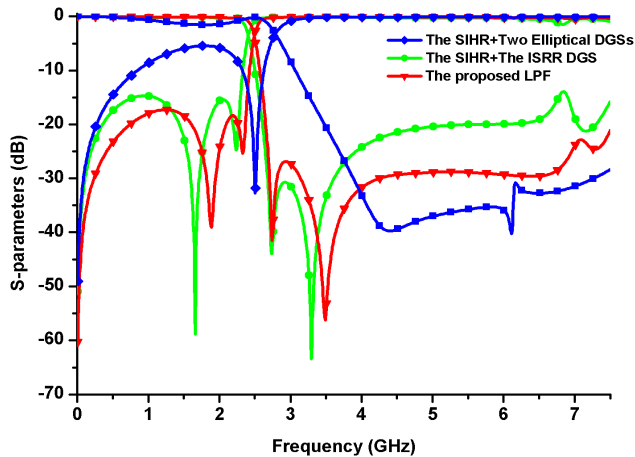
Figure 10. Comparison of the SIHR LPF with different DGS cells.
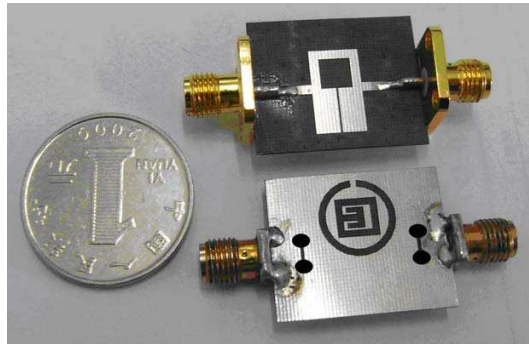
(a)
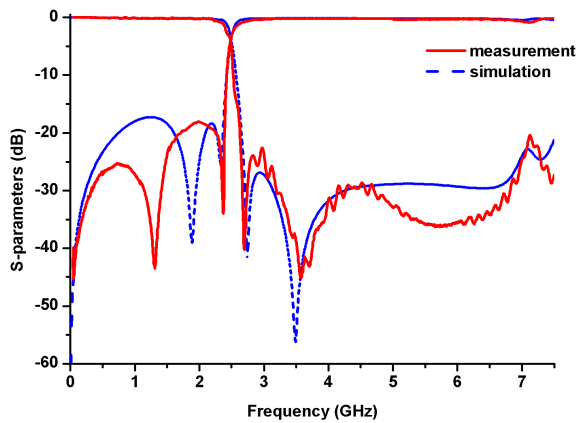
(b)

Figure 11. (a) Photograph and (b) Simulated and measured results of the proposed LPF.

$L_2 = 5.2$ mm, $L_3 = 6$ mm, $L_4 = 5.5$ mm, $L_5 = 3$ mm, $L_6 = 4.56$ mm, $L_7 = 4.5$ mm, $\theta = 5°$. Figure 9 shows the whole view of the proposed LPF.

To comprehensively investigate the influence of two kinds of DGS cells: the elliptical DGS and the ISRR DGS, on the performance of the proposed LPF, different meaningful simulations are performed. That is the performances of the filter composed of the SIHR and the two elliptical DGSs or of the SIHR and the ISRR DGS. Figure 10 shows the simulated result of the SIHR LPF with different types of DGS cells. As shown in the figure, the proposed combination of the two kinds of different DGS units can effectively improve the characteristic of insertion loss at the passband, the cutoff skirts and the attenuation at

the stopband. Factually, the best of the proposed insertion loss is lower than 0.5 dB at the passband, and its attenuation at the stopband better than 20 dB is from 2.58 to 7.5 GHz, which shows a good improvement compared the curve in the Figure 2.

3. MEASURED RESULTS

After the above design and optimization, the proposed LPF is fabricated and measured. Photograph of the proposed filter is shown in Figure 11(a). The measured and simulated results of the return loss are presented in Figure 11(b), which appears a good agreement. Measured result demonstrates the fact that the insertion loss is less than 0.5 dB in the passband, the selectivity of the LPF is more than 100 dB/GHz, and a wide rejected band (lower than 20 dB), from 2.58 to 7.5 GHz, is also achieved.

4. CONCLUSIONS

A compact low-pass filter with DGS is proposed. By adding the ISRR DGS and two elliptical DGSs, the LPF exhibits an excellent characteristic of low insertion loss in the passband, sharp cutoff frequency response and a wide stopband. The characteristic of different DGSs are extensively discussed with its equivalent circuit in this paper. Moreover, the occupied compact size is only $20 \times 25 \, \text{mm}^2$. Both simulated and measured results show that the proposed LPF can be used as a promising candidate for many applications in modern communication systems.

REFERENCES

1. Lim, J. S., J. S. Park, Y. T. Lee, et al., "Application of defected ground structure in reducing the size of amplifiers," *IEEE Microwave Guided Wave Lett.*, Vol. 12, 261–263, 2002.

2. Liu, H.-W., L.-Y. Li, X.-H. Li, and S.-X. Wang, "Compact microstrip lowpass filter using asymmetric stepped-impedance hairpin resonator and slotted ground plane," *Journal of Electromagnetic Waves and Applications*, Vol. 22, No. 11–12, 1615–1622, 2008.

3. Sharma, R., T. Chakravarty, S. Bhooshan, and A. B. Bhattacharyya," Design of a novel 3 dB microstrip backward wave coupler using defected ground structure," *Progress In Electromagnetics Research*, Vol. 65, 261–273, 2006.

4. Ahn, D., J. S. Park, C. S. Kim, Y. Qian, and T. Itoh, "A design of the low pass filter using the novel microstrip defected ground structure," *IEEE Trans. Microwave Theory Tech.*, Vol. 49, 86–93, 2001.

5. Yang, M. H., J. Xu, Q. Zhao, L. Peng, and G. P. Li, "Compact, broad-stopband lowpass filters using SIRS-loaded circular hairpin resonators," *Progress In Electromagnetics Research*, Vol. 102, 95–106, 2010.

6. Yang, M. H., J. Xu, Q. Zhao, and X. Sun, "Wide-stopband and miniarurized lowpass filters using sirs-loaded hairpin resonators," *Journal of Electromagnetic Waves and Applications*, Vol. 23, No. 17–18, 2385–2396, 2009.

7. Park, J. S., J. H. Kim, J. H. Lee, S. H. Kim, and S. H. Myung, "A novel equivalent circuit and modeling method for defected ground structure and its application to optimization of a DGS low pass filter," *IEEE Int. Microwave Symp. Digest*, Vol. 1, 417–420, 2002..

8. Cho, J. H. and J. C. Lee, "Microstrip stepped-impedance hairpin resonator low-pass filter with defected ground structure," *Microwave Opt. Technol. Lett.*, 405–408, 2006.

9. Fu, S., C. Tong, X. Li, W. Zhang, and K. Shen, "Compact miniaturized stepped-impedance lowpass filter with sharp cutoff characteristics," *Microwave Opt. Technol. Lett.*, 2257–2258, 2009.

10. Wu, B., B. Li, and C. Liang, "Design of low-loss filter using novel split-ring resonator defected ground structure," *Microwave Opt. Technol. Lett.*, Vol. 49, 288–291, 2007.

11. Kuo, J. T., M. J. Maa, and P. H. Lu, "Microstrip elliptic function filters with compact miniaturized hairpin resonators," *Asia-Pacific Microwave Conf. Proc.*, Vol. 2, 860–864, 1999.

12. Garde, I., M. J. Yabar, and C. del Rio, "Sample modeling of dgs to design 1 d-pbg low-pass filters," *Microwave Opt. Technol. Lett.*, Vol. 37, 228–232, 2003.

13. Chen, J., Z.-B. Weng, Y.-C. Jiao, and F.-S. Zhang, "Lowpass filter design of Hilbert curve ring defected ground structure," *Progress In Electromagnetics Research*, Vol. 70, 269–280, 2007.